

## ANALYSIS OF THE MUTUAL INDUCTANCE BETWEEN TWO PARALLEL PLATES FOR THE DETECTION OF SURFACE FLAWS

M. Namkung and C. G. Clendenin  
NASA Langley Research Center  
Hampton, VA 23681

J. P. Fulton and B. Wincheski  
Analytic Services and Materials, Inc.  
Hampton, VA 23666

### INTRODUCTION

There has recently been much effort behind the development of NDE methods applicable to the detection of surface/subsurface flaws in thin metallic structures with a rapid scan capability. One such method, an electromagnetic technique using a current-sheet parallel to the surface of a specimen in order to induce eddy current flow shows a high potential for satisfying the rapid scan requirement stated above. The technique is based on the detection of flaw-induced magnetic field components normal to the specimen surface by an appropriate detection mechanism positioned above the current-sheet as shown schematically in Fig. 1. As indicated in this figure, the current-sheet separates the source of the normal magnetic field components from the detector in such a way that the electric and magnetic properties of the current-sheet can be a major factor affecting the strength of the detected signals. The purpose of the present study is, therefore, to perform a detailed investigation on the effect of the material properties of the current-sheet on the detected signal strength and to establish a simple theoretical model for the detection mechanism.

### EXPERIMENTS

For the present study the main focus was on the effects of two physical parameters; resistivity and thickness of the current-sheet. The materials used for the current-sheets included copper, brass and nonmagnetic stainless steel of various thicknesses. All the current-sheets had the same overall dimensions of  $12.7 \times 30 \text{ cm}^2$ , however, the thickness of the sheets was varied. Two aluminum samples of  $12.7 \times 35 \times 0.1 \text{ cm}^3$  were prepared; one without any defect and the other containing a 12 mm-diameter hole at the center with a fatigue crack which was about 7 mm in length and oriented perpendicular to the longer edge of the plate. An insulating tape was applied to the bottom of the each current-sheet to electrically separate the sample from the current-sheet. A bipolar power supply was used to apply an electric current parallel to the longer edge of the current-sheet. The normal component of the flaw-induced magnetic field was detected by a cylindrical pickup coil 5 mm in diameter.

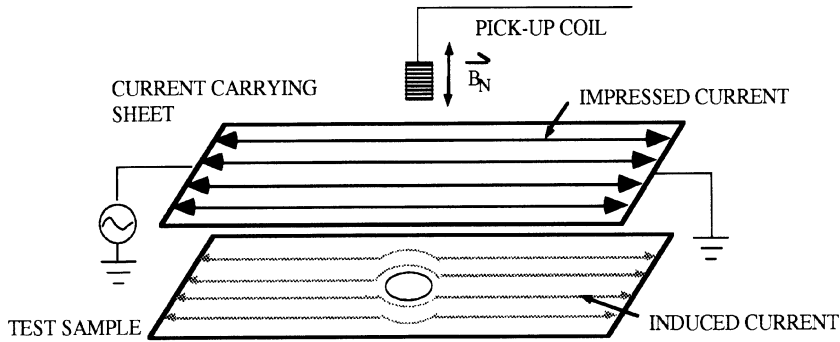


Fig. 1. Schematic of the two plate system with a hole in the sample plate.

10 mm in height and having 3200 turns. A lock-in amplifier was used to measure the RMS value of the pickup coil output. The AC frequency was kept at 30 kHz, and the distance between the top surface of the sample and the bottom surface of the pickup coil was fixed at 2 mm (80 mils) regardless of the current-sheet thickness. The amplitude of the current was fixed at 4.5 amps.

The spatial distribution of the flaw-induced normal magnetic fields was measured by scanning a circular area of 6.8 cm diameter concentric with the 12 mm diameter hole in the sample. The two dimensional scan was performed in steps of 0.12 cm in both the x and y directions.

## RESULTS AND DISCUSSION

Fig. 2a shows the spatial distribution of the normal magnetic field component generated by the current flow in the brass sheet of  $50.8 \mu$  (2 mils) in the absence of a sample. The regions of high field strength are close to the longer edges of the current-sheet where the edge effect is pronounced due to the finite size of the current-sheet. An interesting phenomenon observed is that the slope of the field strength variation from the center to the edge is a decreasing function of both the thickness and the resistivity of the current-sheet. This is certainly related to the current density distribution through the thickness of the sheet and the associated self-inductance of the system, but a detailed analysis has yet to be performed.

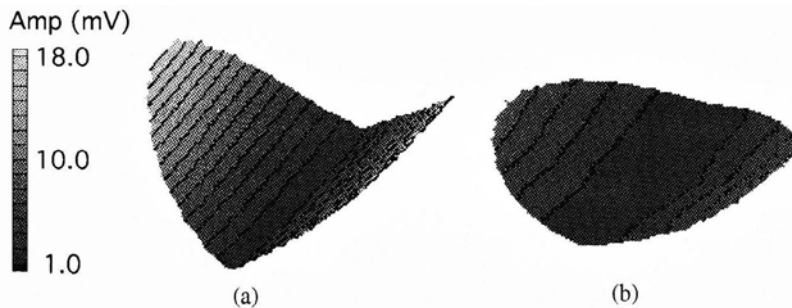


Fig. 2. Spatial distribution of normal component of magnetic fields due to  $50.8 \mu$  thick brass current-sheet (a) without and (b) with a sample.

Placing the sample beneath of the current-sheet should cause a mutual induction between the plates resulting in a reduction in the pickup coil output. This is seen in the results of Fig. 2b which were obtained with the  $50.8\ \mu$  thick brass current-sheet over an aluminum sample without a defect. The pickup coil output clearly shows the expected reduction in the field strength. The results obtained with a sample having a fatigue crack grown at the center hole show a similar edge effect in addition to the flaw-induced normal magnetic field components. The background edge effect of Fig. 2b was subtracted from the results of the sample with a center hole and a fatigue crack to obtain the distribution of the normal component of the flaw-induced magnetic field only.

Fig. 3a shows the background subtracted results of the distribution of the normal component of the flaw-induced magnetic field using the  $5\ \mu$  (2 mils) thick copper current-sheet. The distribution of the normal component of the magnetic field on the left hand side of the center hole is due to the rotational component of the electric currents around the hole. The distribution on the right hand side is extended along the orientation of the fatigue crack. This is because the currents have to detour around the fatigue crack and, as a result, the source of the flaw-induced normal component of the magnetic field is also extended. In addition, there is also a slight reduction in the peak amplitude of the flaw-induced signal. The effect of increasing the thickness of the copper current-sheet to  $15\ \mu$  (6 mils) is shown in Fig. 3b. There is a dramatic reduction in the detected field strength: about a 64% decrease in the strength of peak normal component of the field is obtained by tripling the thickness of the current-sheet. A further increase in the thickness of the copper current-sheet almost completely removes the image of the fatigue crack. Experimentally, this was observed with a copper current-sheet of  $25\ \mu$  (10 mils).

The two-dimensional cross-section of the distribution of the flaw-induced normal magnetic field component is shown in Fig. 4 for pickup coil outputs of 2, 4 and 6 mV. The results in this figure apparently provide the same information on the crack size and orientation as that obtained by a magneto-optic instrument[1]. From the results of Fig. 3a, it is apparent that the image of the flaw can be either focused or defocused in the two-dimensional representation by adjusting the threshold of the normal component of the magnetic field, i. e., moving the plane of view along the vertical axis.

Fig. 5 shows the background subtracted image of the fatigue crack obtained by using  $5\ \mu$  (2 mils) and  $77.5\ \mu$  (31 mils) thick nonmagnetic stainless steel current-sheets, respectively. The results of these tests indicate that the peak amplitude of the normal component of the magnetic field was reduced by less than 10% when the thickness of the stainless steel current-sheet was increased by more than 15 times, while a 64% reduction was observed by

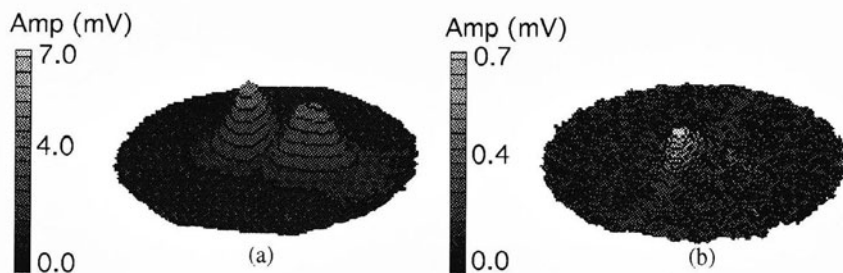


Fig. 3. Background subtracted image of a center hole and fatigue crack obtained by using (a) a  $5\ \mu$  and (b) a  $15\ \mu$  thick copper current-sheet.

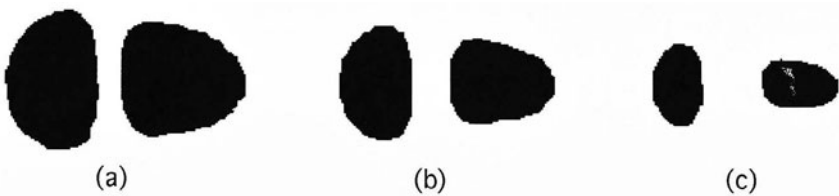


Fig. 4. Two-dimensional cross-section of the equipotential lines taken from the distribution of Fig. 3a at pickup coil outputs of 2, 4 and 6 mV.

increasing the thickness of the copper current-sheet by only a factor of three. An immediate explanation for such a difference in the thickness dependence of the current-sheet is, of course, the skin depth effect of a conductor.

One can argue that, having the source of the normal component of the magnetic field and the detector separated by the current-sheet, the strength of the detected signals will be reduced nonlinearly due to skin depth attenuation which is directly related to the thickness and the conductivity of the current-sheet. At 30 kHz, however, the skin depth for copper is approximately  $38 \mu$  (15 mils), thus, one would only expect a net reduction of about 20% of the signal amplitude by using a  $15 \mu$  as opposed to a  $5 \mu$  copper current-sheet. The experimentally observed signal was about four times smaller than that predicted by the skin depth effect, suggesting that another cause may be responsible for the attenuation. The change in the signal amplitude due to varying the thickness of the stainless steel was less than 10%, but using the skin depth formulation a decrease of about 20% was expected. Again, this suggests that another phenomenon may be responsible for reducing the signal.

The flow of electric and magnetic fields is governed by the electromagnetic wave equation. In a conductor at relatively low frequencies the wave equation reduces to a diffusion equation. The mathematical expression for the skin depth of a conductor is derived from this diffusion equation for an infinite half-space conductor[2,3] and, therefore, is not expected to be directly applicable to the results of the present experiments. In addition, since the thickness of the current-sheets are much smaller than the dimensions of the pickup coil, the effect of the skin depth-induced attenuation of the field strength cannot be assessed with reasonable accuracy. It was expected that the frequency dependence of the detected strength of the normal component of the magnetic field would provide useful information but a series of systematic experiments is yet to be performed. A simple model has been devised to qualitatively explain the experimental results and is presented in the next section.

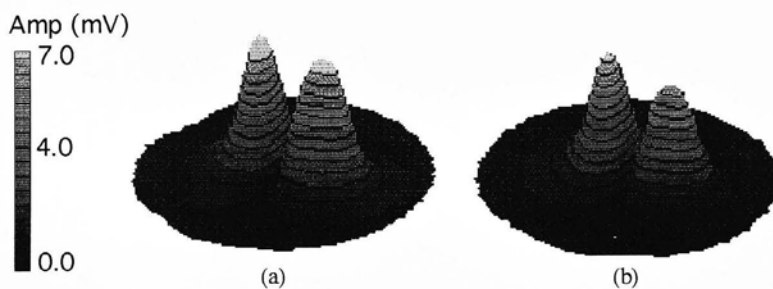


Fig. 5. Background subtracted image of a center hole and fatigue crack obtained by (a) a  $5 \mu$  and (b) a  $77.5 \mu$  thick stainless steel current-sheet.

## EDDY CURRENT IMAGE METHOD

If the time rate of change in an electromagnetic system is sufficiently slow such that the displacement current can be neglected, the expression of Faraday law is as follows:

$$\nabla \times \bar{E} = -\frac{\partial \bar{B}}{\partial t}$$

The electric field can be written in terms of the vector potential as

$$\bar{E} = -\frac{\partial \bar{A}}{\partial t}$$

If the electric field is produced in a conductor a current will flow according to Ohm's law and the following relationship applies:

$$\tau \bar{j} = -\frac{\partial \bar{A}}{\partial t}$$

where  $\tau$  is the resistivity of the conductor. Now consider a vector potential  $\bar{A}(\bar{r}, t)$  associated with the current  $\bar{j}(\bar{r}, t)$  which is induced in a thin conducting sheet, by the action of an external vector potential  $\bar{A}'(\bar{r}, t)$ . The conducting sheet is oriented parallel to the x-y plane and has an area resistivity  $\kappa$ . The electric field is exactly matched by the surface charge such that  $\nabla \cdot \bar{E} = \rho$ . The field created by these surface charges, however, will exactly oppose the original field that produced the charges so that inside the sheet we only need to consider the tangential components of the vector potentials,  $\bar{A}'_t$  and  $\bar{A}_t$ . Hence we may write

$$-\frac{\partial}{\partial t}(\bar{A}'_t + \bar{A}_t) = \kappa \bar{j}$$

Letting the eddy currents be confined to a finite region of the conducting sheet which may or may not extend to infinity, and using a two-dimensional potential and an appropriate stream function, one can show that

$$\frac{\partial}{\partial t}(\bar{A}'_t + \bar{A}_t) = \frac{2\kappa \partial \bar{A}_t}{\mu_v \partial z}$$

The right hand side of the above equation is finite such that as  $\delta t \rightarrow 0$ ,  $\delta(\bar{A}'_t + \bar{A}_t) \rightarrow \bar{0}$ . This means that the following relationship is always valid:

$$\delta \bar{A}'_t = -\delta \bar{A}_t$$

Hence, the effect of the eddy currents induced in the sheet is to produce  $\delta \bar{A}_t$  such that  $\delta \bar{A}'_t + \delta \bar{A}_t = \bar{0}$ , and at any point in and below the sheet no magnetic effects due to  $\delta \bar{A}'_t$  are generated. At the surface of the sheet and at all points in the lower half-space ( $z < 0$ ), the effect of the eddy currents induced on the surface of the sheet is exactly opposite to that of a source positioned at an appropriate point in the upper half-space ( $z > 0$ ). This means that at any point  $z < 0$  the effect of currents in the sheet is equivalent to having an image of the magnetic system (source of  $\delta \bar{A}'_t$ ) coinciding in position with that system but opposite in sign. This can be defined as the eddy current image[4,5].

It is easy to prove that the normal component of the magnetic field on an ideal conducting sheet remains constant in time. If an abrupt change in the normal component of the

magnetic field on the surface of conducting sheet is made by an external means, the eddy currents induced on the surface will be in the direction such that the original magnetic state is preserved. In an ideal conductor with infinite conductivity the strength of the induced eddy currents remain unchanged indefinitely and the effect of  $\delta\bar{A}'$  will never be seen on the other side of the sheet. The eddy currents in a real conducting sheet with a nonzero resistivity, however, do not persist indefinitely but decay exponentially. This means that perfect shielding is only accomplished at the moment  $t=0$  when  $\delta\bar{A}'$  is introduced, but afterward the strength of the eddy current image diminishes. The situation is schematically illustrated in Fig. 6 for the case of a step function for  $\bar{A}'(t)$ .

The actual variation of  $\bar{A}'(t)$  is, of course, a continuous function which can be broken into a series of step functions with duration  $\delta t$  as shown in Fig. 7. Due to the decay of the eddy currents the effect of  $\bar{A}'(t)$  will not be completely cancelled out and the change in the source will be detected on the other side of the sheet as illustrated in Fig. 7.

The simple concept of a decaying eddy current image discussed above is directly applicable to the experimental results obtained for the copper and stainless steel current-sheets. We take the eddy current flowing around the flaw in the sample as the source of  $\bar{A}'(t)$ . This generates the eddy current on the current-sheet which, in turn, generates  $\bar{A}(t)$  that tends to cancel the effect of the time-varying magnetic system on the opposite side of the current-sheet. The conductivity of the current-sheet is finite, therefore, a total cancellation is not accomplished and the detector sees a time-varying field which has been detected. The resistivity of the stainless steel current-sheet is considerably larger than that of copper current-sheet and the eddy current-decay will be much more pronounced. This is why the peak amplitude of the normal component of flaw-induced magnetic field is considerably higher for stainless steel as compared to copper when the current-sheet thickness is the same. For the same material an increase in the thickness will also decrease the area resistivity which results in a slower decay of the eddy currents which reduces the uncanceled effect of  $\bar{A}'(t)$  the detectable. Clearly, the experimental results are seen to be consistent with the effect of a decaying eddy current image.

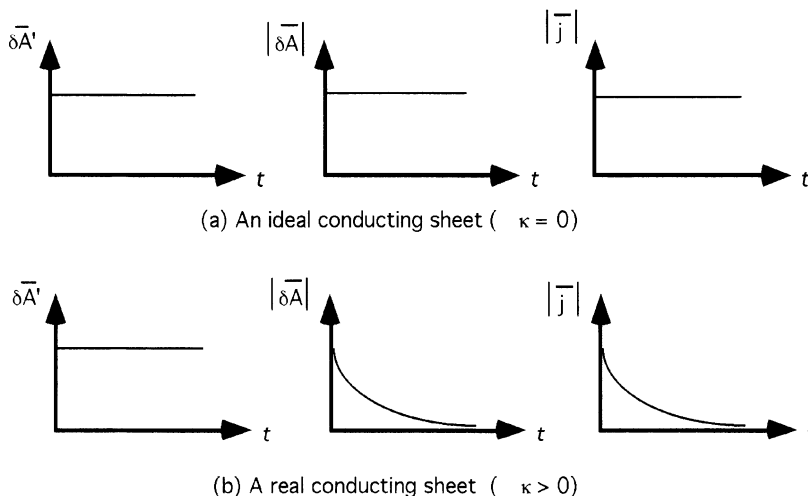


Fig. 6. a. step function for  $\delta\bar{A}'$ ,  $|\delta\bar{A}|$  and  $|\bar{j}|$  for an ideal conductor  
 b. step function for  $\delta\bar{A}'$ ,  $|\delta\bar{A}|$  and  $|\bar{j}|$  for a real conductor

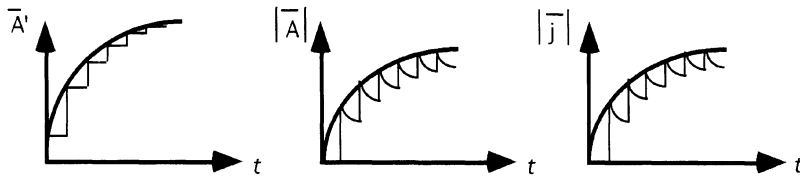


Fig. 7.  $\bar{A}'(t)$ ,  $|\bar{A}|$  and  $|\bar{j}|$  all broken into small intervals

## SUMMARY

A series of experiments were performed to investigate the effect of electrical conductivity and the thickness variations of a current-sheet on the strength of the normal component of flaw-induced magnetic fields detected by an induction pickup coil. It was shown that the experimental results are consistent with a simple model based on the eddy current image method and its decay is governed by the electrical conductivity and thickness of the current-sheet. More details of the model, however, need to be worked out to make a truly quantitative assessment of the experimental results such that the capabilities of the technique can be maximized.

## REFERENCES

1. B. Wincheski., D. R. Prabhu., M. Namkung, and E.A. Birt, "Imaging Flaws in Thin Metal Plates Using a Magneto-Optic Device," *Review of Progress in Quantitative NDE*, Vol. 11a, edited by D.O Thompson and D.E. Chimenti (Plenum Press, New York, 1992). pp. 879-886.
2. J. D. Jackson, *Classical Electrodynamics*, 2nd edn, John Wiley & Sons, Inc., New York, 1976.
3. H.L. Libby, *Introduction to Electromagnetic Nondestructive Test Methods*, John Wiley & Sons, Inc., New York, 1971.
4. W.R. Smythe, *Static and Dynamic Electricity*, 2nd edn, McGraw-Hill Book Company, Inc., New York, 1950.
5. J. C. Maxwell, *A Treatise on Electricity and Magnetism*, Vol. II 3rd edn, Oxford University Press, London, 1892.